

Tangent map for classical billiards in magnetic fields

This article has been downloaded from IOPscience. Please scroll down to see the full text article.

1993 J. Phys. A: Math. Gen. 26 237

(<http://iopscience.iop.org/0305-4470/26/2/012>)

View [the table of contents for this issue](#), or go to the [journal homepage](#) for more

Download details:

IP Address: 171.66.16.68

The article was downloaded on 01/06/2010 at 19:47

Please note that [terms and conditions apply](#).

Tangent map for classical billiards in magnetic fields

O Meplan, F Brut and C Gignoux

Institut des Sciences Nucléaires, F-38026 Grenoble Cédex, France

Received 6 April 1992, in final form 9 September 1992

Abstract. A charged particle is moving inside a planar billiard embedded in a uniform constant magnetic field which is directed perpendicular to the plane. The stability of classical trajectories is studied by the area-preserving tangent map which is derived for any billiard shape having a smooth convex boundary. As an example, two generic billiards are considered here, namely the ellipse and the stadium, classical trajectories of which are well known to be regular or chaotic, respectively, for an uncharged particle. Lyapunov exponents and Poincaré sections are studied as a function of the field strength and of the billiard deformation. Regular motion is restored by increasing the magnetic field and/or the deformation.

1. Introduction

There are only a few cases in which dynamical systems can be reduced to mappings which remain useful in characterizing chaotic or regular motions. Moreover, the classification of fixed points and the studies of the stability of classical trajectories are easily understood by the properties of a linearized version of the mapping, often referred to as the tangent map. In this work, we will show how to derive analytically the tangent map for a charged particle moving in a planar billiard which is embedded in a uniform perpendicular magnetic field. Of course, the mapping itself, which gives the location on the boundary of the successive bounces of the particle and the orientation of its velocity, is only determined numerically. The tangent map, we found, generalizes a previous result obtained by Berry (1981) for a particle bouncing in a billiard without any magnetic field.

Classical magnetic billiards were first studied through the geometry of classical orbits by Robnik and Berry (1985). These simple systems are interesting from a quantum point of view because the magnetic field breaks the time reversal symmetry and yields new properties of the level spacings (Berry and Robnik 1986, Robnik and Berry 1986). Billiards in magnetic fields are also studied in connection with more general phenomena in condensed matter physics, such as the diamagnetic susceptibility, when the Larmor radius is close to the dimensions of the billiard (Nakamura and Thomas 1988).

In this work, we will derive the tangent map for a charged particle inside a smooth convex billiard in a constant perpendicular magnetic field. The tangent map will be used to calculate the Lyapunov exponent of any classical trajectories in connection with Poincaré sections for two particular billiard shapes: the ellipse and the stadium. Without any magnetic field, the former is an integrable system, the latter is an ergodic system. Therefore, it would be interesting to see how the chaotic motion could be enhanced by the magnetic field, on one hand, or how the order could be restored by increasing either the deformation or the field strength.

2. Derivation of the tangent map

We consider a unit mass particle with an electric charge q , moving with the velocity v inside a planar billiard. If this billiard is embedded in a constant magnetic field of strength B perpendicular to the plane of the billiard, the classical trajectories of the particle are made of arcs of a circle, the radius of which is the Larmor radius given by

$$R = \frac{v}{qB} = \frac{v}{|\omega|} \quad (1)$$

where ω , the angular velocity of the motion, is parallel to the z axis which is perpendicular to the billiard plane. The geometry of the mapping is shown in figure 1, where the particle starts in M_0 on the billiard boundary, with a velocity v_0 . The tangent t_0 to the boundary (anticlockwise orientated) at M_0 is used to define the angles

$$(\overline{Ox}, t_0) = \psi_0 \quad (t_0, v_0) = \alpha_0 \quad (2)$$

where \overline{Ox} is any direction in the plane of the billiard. The corresponding angles ψ_1 and α_1 are defined in M_1 which is the next bounce on the boundary for the trajectory starting in M_0 . We choose two particular directions in the plane of the billiard, u is a unit vector parallel to $\overline{M_0M_1}$, and r is perpendicular to u , the reference frame (u, r, k) being a direct trihedral. Between M_0 and M_1 , the velocity v turns around C by an angle 2φ , defined by

$$(u, v_0) = \varphi. \quad (3)$$

The tangent map is obtained by considering the following invariant between two successive bounces:

$$v_0 - \omega \wedge \overline{OM_0} = v_1 - \omega \wedge \overline{OM_1}. \quad (4)$$

As the velocity modulus is conserved along the trajectory, the variation of the preceding

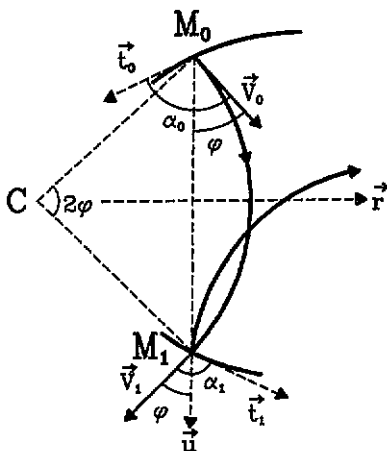


Figure 1. Geometry and definitions of the convex billiard in a magnetic field. One trajectory is shown here, starting in M_0 on the boundary with a unit velocity v_0 .

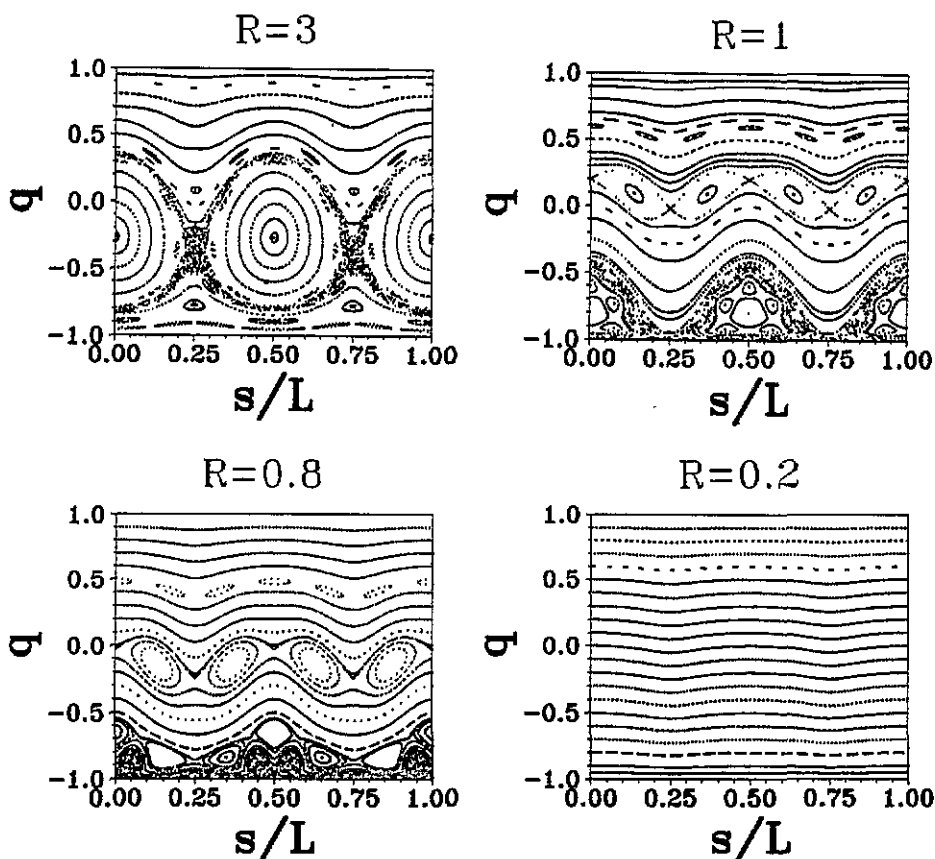


Figure 2. Poincaré sections for an elliptic billiard of deformation $\mu = 1.25$ in magnetic field (the deformation μ is the semi-axis ratio of the elliptic boundary). q is the projection of the velocity on the tangent of the boundary when the particle hits it, s is the curvilinear abscissa on the ellipse, L is the perimeter of the ellipse and R is the Larmor radius.

equation gives

$$(d\alpha_0 + d\psi_0)\mathbf{k} \wedge \mathbf{v}_0 - ds_0 \boldsymbol{\omega} \wedge \mathbf{t}_0 = (d\alpha_1 + d\psi_1)\mathbf{k} \wedge \mathbf{v}_1 - ds_1 \boldsymbol{\omega} \wedge \mathbf{t}_1. \quad (5)$$

By projecting equation (5) on the directions \mathbf{u} and \mathbf{r} , we obtain

$$\begin{bmatrix} \frac{1}{\rho(\psi_0)} - \frac{\sin(\alpha_0 - \varphi)}{R \sin \varphi} & 1 \\ \frac{1}{\rho(\psi_0)} + \frac{\cos(\alpha_0 - \varphi)}{R \cos \varphi} & 1 \end{bmatrix} \begin{bmatrix} ds_0 \\ d\alpha_0 \end{bmatrix} = \begin{bmatrix} -1 - \frac{\sin(\alpha_1 + \varphi)}{R \sin \varphi} \\ \frac{1}{\rho(\psi_1)} + \frac{\cos(\alpha_1 + \varphi)}{R \cos \varphi} \end{bmatrix} \begin{bmatrix} ds_1 \\ d\alpha_1 \end{bmatrix} \quad (6)$$

where we introduced the radii of curvature in M_0 and M_1 , $\rho(\psi_0)$ and $\rho(\psi_1)$ respectively, defined by

$$\rho(\psi) = \frac{ds}{d\psi}. \quad (7)$$

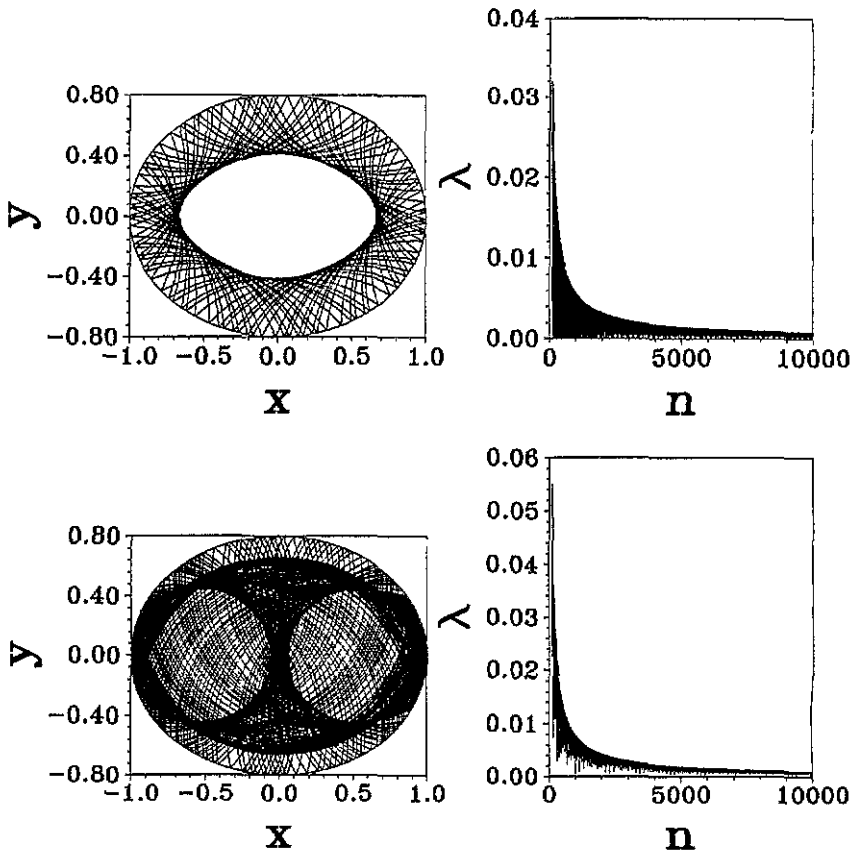


Figure 3. Regular classical trajectories in the x - y plane of the elliptic billiard and their corresponding Lyapunov functions λ , versus the number n of successive bounces, for a deformation $\mu = 1.25$ and a Larmor radius $R = 1$.

A straightforward calculation shows that the two matrices appearing in equation (6) have the same determinant if we change the variable α to $q = \cos \alpha$, as done by Berry (1981). By inverting one of the matrices, we finally obtain:

$$\begin{bmatrix} ds_1 \\ dq_1 \end{bmatrix} = \begin{bmatrix} \frac{\sin(\alpha_0 - 2\varphi)}{\sin \alpha_1} - \frac{R \sin 2\varphi}{\rho(\psi_0) \sin \alpha_1} \\ \frac{\sin(\alpha_0 - 2\varphi)}{\rho(\psi_1)} - \frac{R \sin 2\varphi}{\rho(\psi_0)\rho(\psi_1)} - \frac{\sin(\alpha_1 + 2\varphi)}{\rho(\psi_0)} - \frac{\sin(\alpha_1 + 2\varphi - \alpha_0)}{R} \\ \frac{R \sin 2\varphi}{\sin \alpha_0 \sin \alpha_1} \\ \frac{R \sin 2\varphi}{\rho(\psi_1) \sin \alpha_0} + \frac{\sin(\alpha_1 + 2\varphi)}{\sin \alpha_0} \end{bmatrix} \begin{bmatrix} ds_0 \\ dq_0 \end{bmatrix}. \quad (8)$$

The determinant of the matrix (T) given by equation (8) is then unity and thus the mapping is area preserving. If we want to connect the deviations (ds_1, dq_1) when the

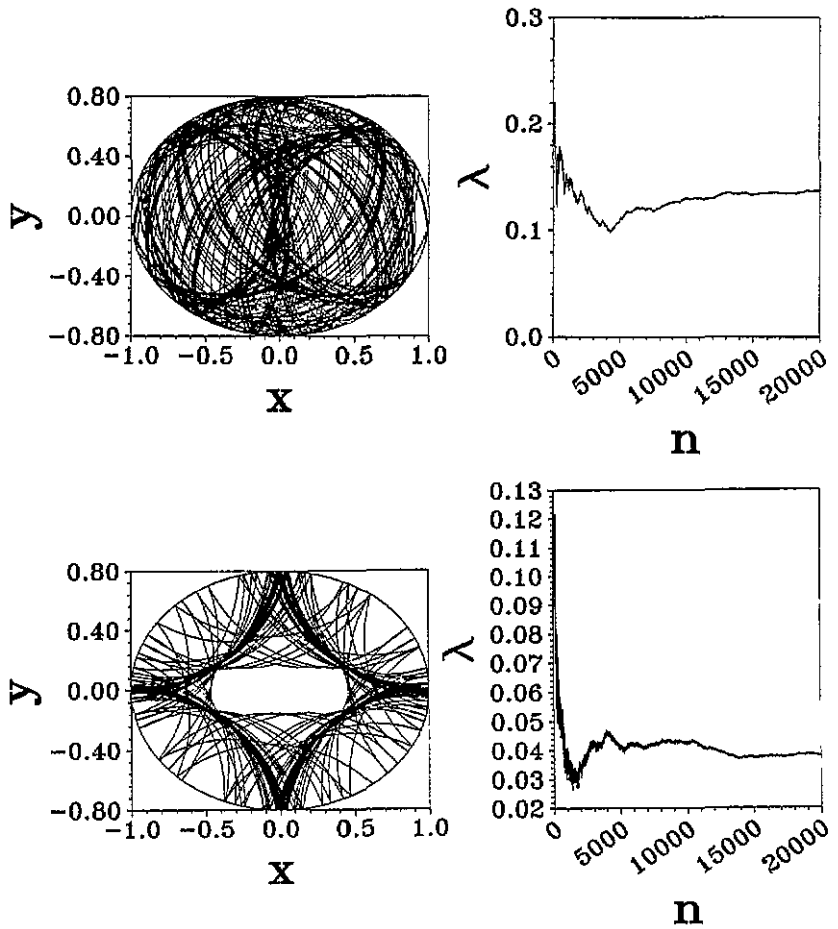


Figure 4. Same as figure 3 but for two chaotic trajectories.

perfect reflection in M_1 is done, i.e. after returning the velocity v_1 with respect to the tangent t_1 (see figure 1), we have to change α_1 in $-\alpha_1$ in the matrix defined by equation (8).

Of course, when the magnetic field is vanishing, the deviation matrix given by equation (8) has the limit already found by Berry (1981), for the motion of a free particle inside a convex billiard. Indeed, when the field strength B is vanishing, then the Larmor radius R goes to infinity and the angle φ is going to 180° but

$$\lim_{B \rightarrow 0} R \sin 2\varphi = \rho_{01} = M_0 M_1. \tag{9}$$

Another interesting limit is that of a circular billiard in magnetic field. The classical motion is then integrable. Beside the energy conservation, a second constant of motion can be found; in this case, we noticed that the angles α_n for the n th bounce have the following property:

$$\alpha_n = \text{constant for a circular billiard.} \tag{10}$$

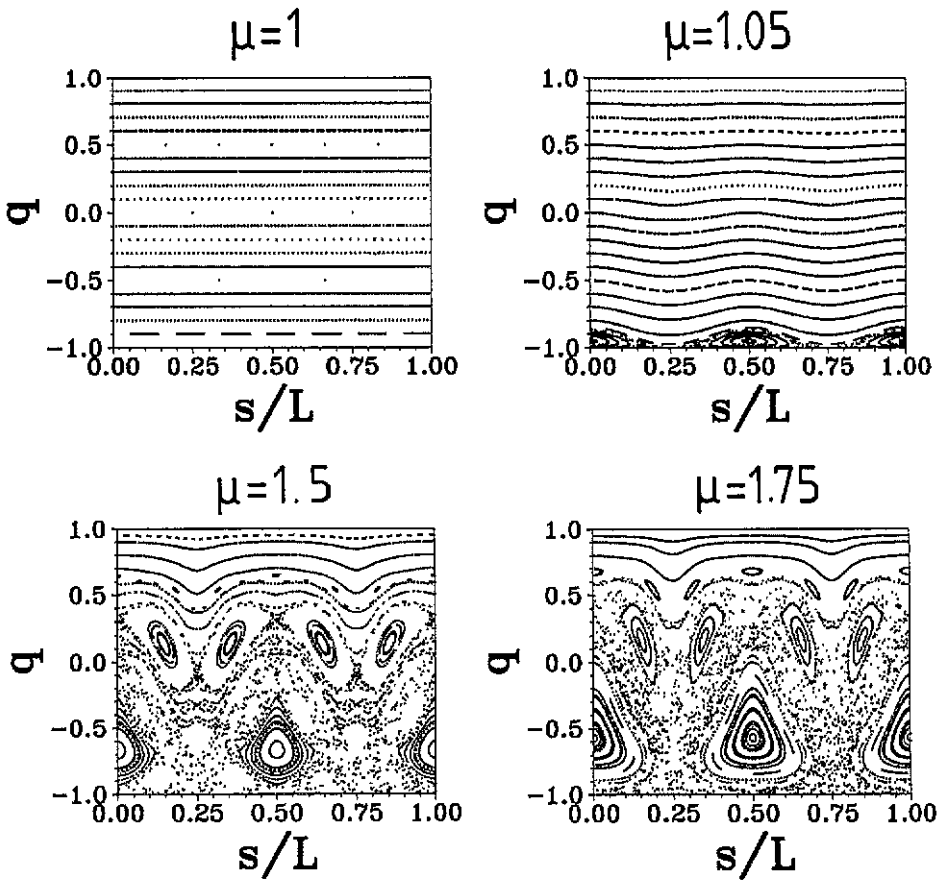


Figure 5. Poincaré sections for an elliptic billiard in a magnetic field for different values of the deformation μ and for a Larmor radius $R = 1$.

For a billiard of any smooth convex shape, the tangent map allows us to calculate the Lyapunov exponent associated to each classical trajectory. If we consider a reference trajectory starting in M_0 with the variables (s_0, q_0) and a second trajectory starting from M'_0 with variables $(s_0 + \delta s_0, q_0 + \delta q_0)$ where δs_0 and δq_0 are infinitely small, then after N bounces of the particle on the boundary the deviations δs_N and δq_N will be

$$\begin{bmatrix} \delta s_N \\ \delta q_N \end{bmatrix} = (T)_{N,N-1} (T)_{N-1,N-2} \dots (T)_{1,0} \begin{bmatrix} \delta s_0 \\ \delta q_0 \end{bmatrix} \quad (11)$$

where the matrix $(T)_{i,i-1}$ is connecting two successive deviations corresponding to the $(i-1)$ th and i th bounces on the boundary. The matrix elements of the matrix $(T)_{i,i-1}$ are given by equation (8) and depend on the curvilinear coordinates s of the successive bounces on the boundary, the orientations of the velocity with respect to the tangent on the boundary and the curvature radii at the bounce. As each matrix in equation (11) has a unit determinant, if the trace of the product matrix is greater or less than 2, the corresponding trajectory is chaotic or regular, respectively (see Berry 1981). Indeed, the Lyapunov exponents are just the infinite time-limit of the logarithm of the eigenvalues of the product matrix and therefore have opposite values as the mapping is area preserving.

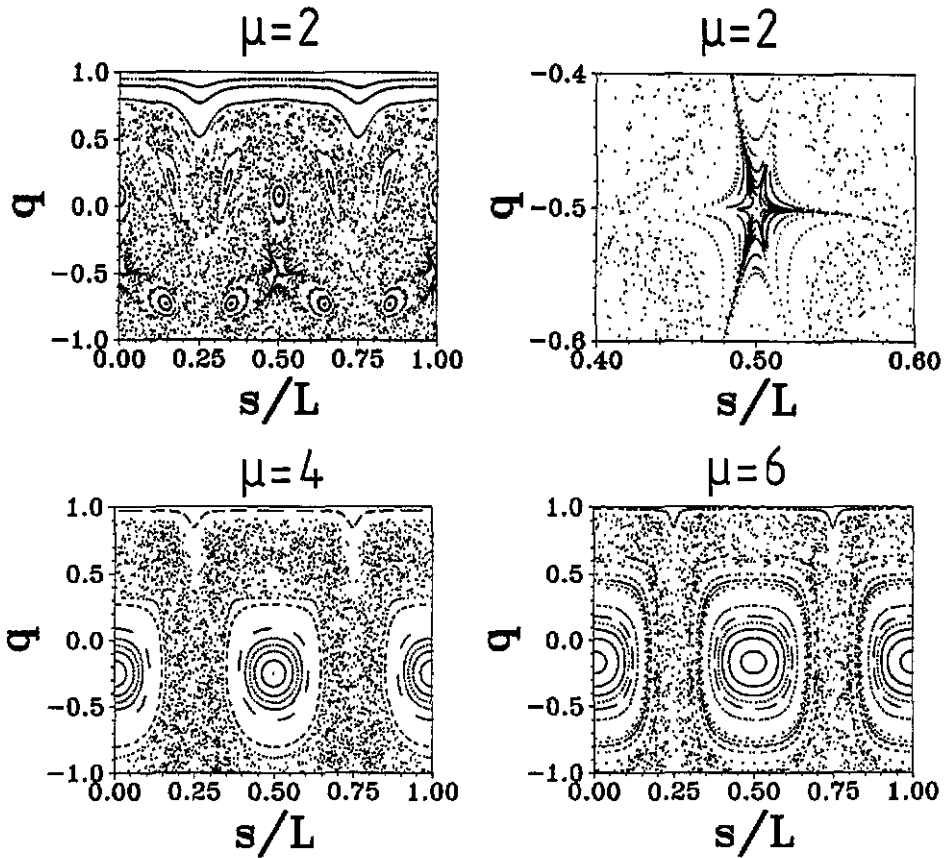


Figure 5. (continued).

In the following, two specific cases will be considered, the elliptic billiard and the stadium. Without any magnetic field the former is an integrable system, the latter an ergodic one. Introducing a magnetic field will break these general properties and will be studied as a function of the field strength and the billiard deformation.

3. Ellipse and stadium in a magnetic field

In this section, we present the Lyapunov exponent calculations using the tangent map and the Poincaré sections for two billiards in a magnetic field: the ellipse and the stadium. For the elliptic billiard, we define the deformation by $\mu = a/b$, where a and b are respectively the semi-major and semi-minor axis of the ellipse. For the stadium, the shape parameter γ is defined by the ratio of the straight segment to the diameter of the half-circles.

Figure 2 shows Poincaré sections for an ellipse with deformation $\mu = 1.25$ and for various magnetic field strengths B . For a vanishing magnetic field, the classical motion is integrable and only two topologies are present in the phase space: one is made by the classical trajectories which never cross the segment between the two foci, the second by the trajectories which cross the foci segment. Therefore, a separatrix exists in this case, and, as expected, when the field strength B is small but non-vanishing, the chaotic

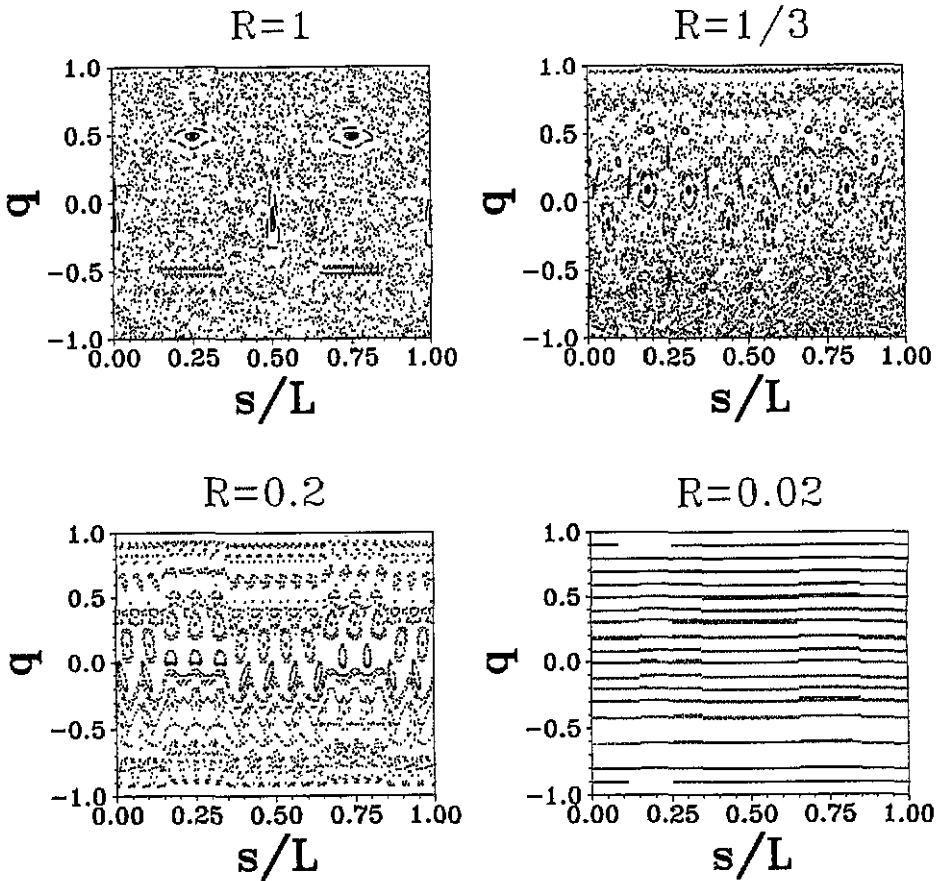


Figure 6. Poincaré sections for a stadium in a magnetic field. The shape parameter of the stadium is $\gamma = 1$ in all the cases, R is the Larmor radius.

motion is first developing, on a macroscopic scale, around the separatrix (see for example figure 2 for $R = 3$). When B is increasing, the chaotic trajectories correspond mainly to an orientation of the velocity, versus the tangent on the boundary, close to π . As the magnetic field strength B is increasing, the chaotic region is shrinking at an increasing rate and totally disappears for the largest value of B , restoring a regular motion everywhere in the phase space. Figure 3 shows two different classical trajectories corresponding to a regular motion. The corresponding evolution of the Lyapunov function versus the number of bounces n is shown on the right-hand part of figure 3. Lyapunov functions are evaluated by using the tangent map given by equation (8). The general behaviour of the Lyapunov functions for these regular trajectories is very similar to that already observed for the regular trajectory of a hydrogen atom in a magnetic field (Schweizer *et al* 1988). Figure 4 shows two classical trajectories and their Lyapunov exponents when the initial conditions are taken in the chaotic region, for a magnetic field strength B corresponding to a Larmor radius $R = 1$ and an ellipse deformation $\mu = 1.25$. Now, the Lyapunov functions reach asymptotically a constant value, different from zero, even if it is somewhat difficult to precisely determine this value. In figure 5, different Poincaré sections are shown for the elliptic billiard in a

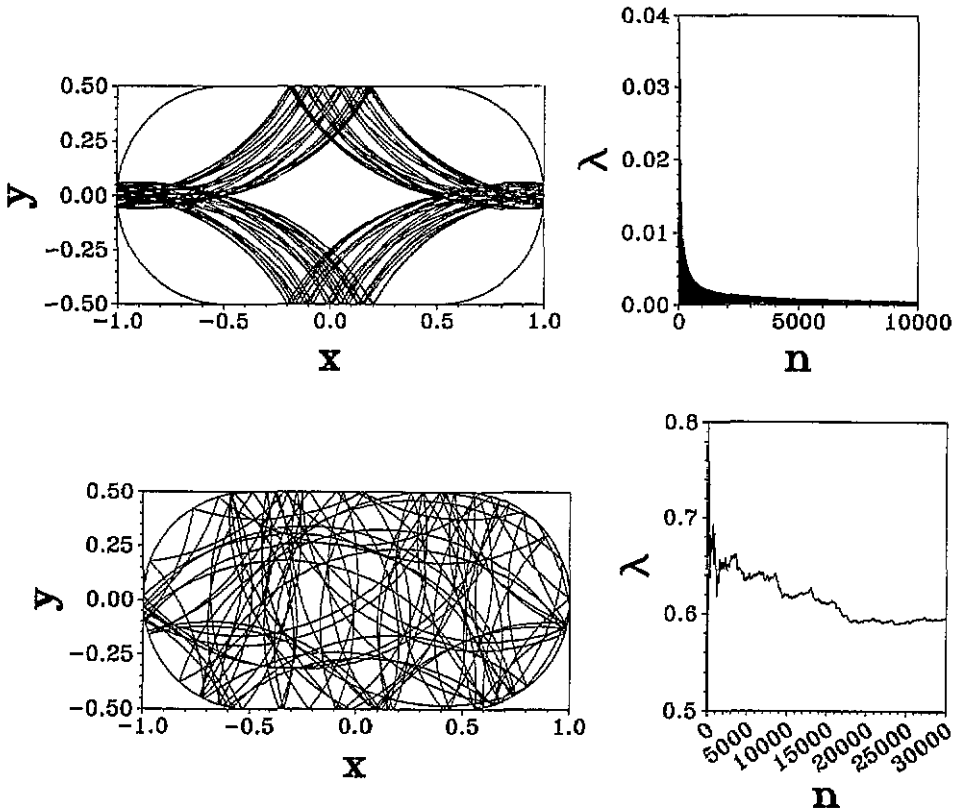


Figure 7. Regular (top) and chaotic (bottom) trajectories in a stadium with a shape parameter $\gamma=1$ and a Larmor radius $R=1$. Each trajectory is drawn for the first 100 bounces on the boundary. The corresponding Lyapunov function λ is plotted versus the number n of successive bounces of the particle.

magnetic field, corresponding to different values of the deformation μ and a constant field strength. The area of the ellipse is kept constant when the deformation is varying. In a circular billiard, shown in figure 5 for $\mu=1$, any condition corresponds to a regular trajectory, as already underlined by equation (10). When the deformation is small— $\mu=1.05$ in figure 5—the chaotic motion appears for an angle α , between the velocity and the tangent to the boundary, close to π . When the deformation increases for a constant magnetic field, the chaotic region is expanding except for trajectories close to the periodic orbit around the semi-minor axis and for an angle α close to zero. For $\mu=2$, the chaotic region is well developed even if a careful analysis of the Poincaré section shows a fixed point for $(s/L, q) \equiv (\frac{1}{2}, -\frac{1}{2})$ (see the enlarging part surrounding this point on figure 5). For a larger deformation, order is restored and the chaotic region is smoothly shrinking but great values of μ ($\mu > 6$) are needed to reach a complete order. Therefore in order to summarize, increasing the field strength for a fixed deformation of the elliptic billiard favours the appearance of chaotic motion which reaches a maximum before disappearing at large values of the magnetic field. The same conclusion is obtained by keeping a constant magnetic field and by increasing the deformation of the ellipse.

It is interesting to see what the changes are if we take an opposite starting point for the billiard shape. Instead of an integrable system, as the ellipse, let us start with an ergodic system, the stadium. The deformation γ is defined by the ratio of the straight section length and the circle diameter of the stadium. Figure 6 shows four Poincaré sections, corresponding to a stadium having a shape parameter $\gamma = 1$, for different magnetic field strengths B . For the smallest values of B , the Poincaré sections are filled by chaotic trajectories except for small regions which correspond to periodic trajectories bouncing between the two straight lines of the billiard. For the largest values of B , order is restored and the shape of the billiard has almost no influence on the general form of the Poincaré sections as can be seen, for the ellipse and the stadium, by comparing $R = 0.2$ in figure 2 and $R = 0.02$ in figure 6, respectively. Figure 7 shows the evolution of the Lyapunov exponent for a regular and a chaotic trajectory, in a stadium embedded in a constant magnetic field, as a function of the number of bounces of the particle on the boundary. The Lyapunov evolutions are similar to the corresponding quantities in an elliptic billiard, see for example figures 3 and 7 for regular trajectories, and figures 4 and 7 for chaotic trajectories. In this latter case, the asymptotic value reached by the Lyapunov exponent is greater for the stadium than for the ellipse. Extensive use of the tangent map given by equation (8), allows us to compute very easily the Lyapunov exponent without considering two trajectories which are initially nearby as proposed by Benettin *et al* (1976).

4. Summary and conclusion

In this work, we derived the analytical expression of the tangent map corresponding to the classical motion of a charged particle in a planar billiard embedded in a constant uniform magnetic field perpendicular to the plane. The billiard must have a smooth convex boundary. The tangent map is a 2×2 matrix, the elements of which are functions of the magnetic field, the successive curvilinear coordinates, the scalar products of the velocity with the tangent on the boundary and the curvature radii at each bounce. For a vanishing value of the magnetic field, this tangent map has the limit already found by Berry (1981). The properties of this mapping are extensively used in the calculation of the Lyapunov exponents for two billiard shapes: the ellipse and the stadium. The former is an integrable system for a vanishing magnetic field while the latter is an ergodic system. Finally, it is shown that increasing either the field strength or the deformation of the billiard, keeping the area of the billiard constant, is followed by the appearance of large chaotic regions in the phase space which are disappearing when great values of these two parameters are reached.

References

- Benettin G, Galgani L and Strelcyn J M 1976 *Phys. Res. A* **14** 2338
 Berry M V 1981 *Eur. J. Phys.* **2** 91
 Berry M V and Robnik M 1986 *J. Phys. A: Math. Gen.* **19** 649
 Nakamura K and Thomas H 1988 *Phys. Rev. Lett.* **61** 247
 Robnik M and Berry M V 1985 *J. Phys. A: Math. Gen.* **18** 1361
 ——— 1986 *J. Phys. A: Math. Gen.* **19** 669
 Schweizer W, Niemeier R, Friedrich M, Wunner G and Ruder H 1988 *Phys. Rev. A* **15** 1724